Applied Energy 358 (2024) 122617

Contents lists available at ScienceDirect

Applied Energy

journal homepage: www.elsevier.com/locate/apenergy

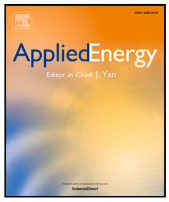

Model predictive control of bidirectional heat transfer in prosumer-based solar district heating networks

Lilli Frison [a,*], Manuel Kollmar [c], Axel Oliva [a], Adrian Bürger [b], Moritz Diehl [d]

[a] Fraunhofer Institute for Solar Energy Systems (ISE), Freiburg, Germany
[b] Institute of Applied Research, Karlsruhe University of Applied Sciences, Karlsruhe, Germany
[c] Institute of Refrigeration, Air-Conditioning and Environmental Engineering (IKKU), Karlsruhe University of Applied Sciences, Karlsruhe, Germany
[d] Systems Control and Optimization Laboratory, Department of Microsystems Engineering (IMTEK), University of Freiburg, Freiburg, Germany

ARTICLE INFO

Keywords:
District heating network
Optimal control
Model predictive control
Bidirectional heat transfer
Prosumer
Decentral heat generation

ABSTRACT

District heating networks with decentralized heat production are ideally suited to include a high share of renewable energy sources for heat production in urban areas with limited space. A new concept is a prosumer-based district heating network in which some or even all buildings are equipped with decentralized building-level heat storages and heat generation plants. To exploit the full potential of the interconnected heating network, buildings with surplus heat are intended to transfer heat to buildings with heating demands to prevent the activation of the central heating plant. This work presents an initial feasibility study on using a model predictive control strategy to manage bidirectional heat transfer between buildings in a district heating network. We formulate this problem as an optimal control problem, incorporating binary decision variables for each potential heat transfer connection. This results in a mixed-integer nonlinear optimization problem that is hard to solve. The problem is solved with a fast gradient-based optimization algorithm in combination with a combinatorial integral approximation strategy. A case study concerning a residential heating network with building-level solar thermal collectors and storage tanks is carried out. The optimized operation is compared to the real operation obtained from one month of measurements. The results show that the optimized strategy with bidirectional heat transfer can exploit the total heat generated in the whole network. The central heating provider is only required when the heat produced or stored by all the buildings is insufficient to meet the total heat demand within the network. In the case study, this leads to a reduction of almost 75% of the required thermal energy from the central heat provider.

1. Introduction

About 40% of the energy consumed in Europe is for heating, most of which, up to date, is provided by fossil fuels. Germany, as well as many European countries, has set the goal to reduce emissions in this sector by 40% by 2030 compared to 1990 to achieve climate targets. Reducing CO_2 emissions in the building heating sector by improving the energy efficiency of the heating system and increasing the share of renewable energy sources plays a significant role [1]. In addition to increasing the energy efficiency of buildings and their heating and cooling systems, smart operation of the heat generation and distribution systems and their components is very important. An urgent challenge for future energy systems is to find a design and operation that makes large amounts of fluctuating renewable energy usable while simultaneously increasing the overall system's efficiency. District heating systems are particularly important in urban areas with limited space for renewable energy generation plants, making smaller decentralized systems advantageous in combination with district heating networks. The important open question is how the decentralized plants can be integrated into the overall system.

1.1. Prosumers-based district heating network

This article concerns the development of smart control of a district heating network in which many or even all buildings act as prosumers – that is, a customer who can both consume and produce heat – and a bidirectional heat exchange between the connected buildings is possible. The considered district heating network is equipped with building-level distributed heat storage and renewable energy plants consisting of a storage tank in each building and a solar thermal collectors on the rooftop. The integration of decentralized solar thermal

* Corresponding author.
E-mail address: lilli.frison@ise.fraunhofer.de (L. Frison).

https://doi.org/10.1016/j.apenergy.2023.122617
Received 13 February 2023; Received in revised form 13 December 2023; Accepted 30 December 2023
Available online 13 January 2024
0306-2619/© 2024 The Authors. Published by Elsevier Ltd. This is an open access article under the CC BY license (http://creativecommons.org/licenses/by/4.0/).

panels with a district heating network combines the strengths of both systems, leading to enhanced economic and environmental outcomes. A typical design of the decentralized solar-thermal system accounts for 60% of the building's domestic hot water demand. This design approach, focusing on optimizing cost-efficiency and CO_2 reduction, allows the solar thermal system to function independently as a heating solution during warm summer periods, without the need for oversizing the system. With special operating modes, such as decentralized heat transfer between buildings, the network is expected to be energy self-sufficient in periods with high renewable energy generation. Consequently, the central heating plant can be turned off during long sunny periods. A simulation by Elci [2] shows that through such an intermittent operation, the heating network can reduce heat distribution losses by up to 30%. Model-predictive control (MPC) can be used to find an optimal control of the central heating plant and to optimally operate a cooperative user-level heat transfer from buildings with heat surplus to buildings with heat demand. It allows the optimal use of the system's energy storage capabilities and optimization of energy production from renewable energy sources. At the same time, constraints on the system limits and comfort requirements are considered. Applying MPC for this task is a challenge that will likely arise more often in future district heating networks.

The possibility to choose between alternative options within the optimization problem leads to discrete decision variables. A common nonlinearity for heating applications is the bilinear relationship between the temperature and mass flow in the energy balance equations. Therefore, district heating networks that consist of multiple alternative heat sources are characterized by having nonlinear continuous-time dynamics and discrete or mixed-integer decision variables. The optimized control of the dynamic system then leads to the formulation of a nonlinear mixed-integer optimal control problem (MIOCP) that is hard to solve.

In our investigation, we also considered the potential development of a heuristic rule-based strategy for bidirectional cooperative heat transfer. The approach involved maintaining lists of buildings characterized by either heat demand or heat surplus, coupled with a priority-based decision-making system to match buildings with heat demand to those with surplus. However, our exploration led to a significant realization: the process of deriving such a rule-based strategy in a robust and automated manner posed challenges comparable to those encountered in creating an optimization-based Model Predictive Control (MPC) strategy. This finding not only highlights the complexity inherent in such systems but also underscores the need for advanced solutions that can effectively manage these complexities.

1.2. Related work

MPC is an established method for optimal control of systems with constraints that combines the principles of feedback control, considering predictions of future behavior of the influencing parameters and of the system and numerical optimization. Many studies have shown the potential of MPC controllers to improve the energy efficiency of the building heating and cooling operation compared to the conventionally used rule-based controllers, e.g., [3,4]. The first mention of MPC in the field of district heating networks can be found in [5]. In this work, the mass flow rate of the pumps and the supply temperature of the heat generator in the district heating network are controlled with several rule-based lower-level controllers, and the MPC acts as the central controller. Currently, the use of MPC for the operational optimization of district heating systems with multiple power generators has received attention in research. The focus is on controlling the centralized heat generation and flexible load management, especially for better integrating volatile renewable energy sources. Some articles deal specifically with the inclusion of renewable energy or waste heat sources, see [6], or a grid-supportive district heating operation. The thermal inertia of the system is used for flexibility and load shifting in the sense of an electricity grid-serving operation. The utilized thermal inertia in a district heating network consists of the thermal storage tanks, the heat transfer fluid, and the thermal mass of the buildings [7,8]. In the work of Vanhoudt et al. [8], the economic efficiency of different configurations of thermal storage in a district heating network with 100 buildings is compared in a reference winter week. First, the heat demand is determined and aggregated via so-called consumer agents. A higher-level MPC then calculates the optimal aggregated power profile, considering the integrated costs for consumed fuel and variable compensation for electricity generation. The optimized power profile is distributed to the properties via the market agent. For the MPC, aggregated models of the thermal storages are used. As a result of the work, it can be stated that distributed storages are most economical. Particularly advantageous due to the low investment costs is the use of the thermal mass of the buildings. In [9,10], the heat generator is controlled with an MPC that considers the building's thermal capacity to avoid peak loads. The optimization problem for MPC is described by a mixed-integer linear program (MILP) in both papers. Aoun et al. [9] estimate the modeling parameters initially with an optimization from three weeks of measured data to keep model errors small. The optimization is discrete due to the discontinuous functions in the cost function for superheating and subcooling, which allow for exploiting flexibility in the room temperature comfort range. This approach is implemented in the modeling language Modelica in combination with GenOpt for the MPC. GenOpt is a stochastic optimization algorithm for arbitrary problem structures, which, however, is not suitable for real-time operational optimization due to its complexity and very slow runtime [11].

Agent-based architectures have also been considered, e.g., in [12]. The particular implementation depends on the heating network's structure and the participants' chosen business model, e.g., centrally controlled or self-regulated and decentrally controlled. In the agent-based approaches, heat loads are modeled as consumer agents and heat generators as producer agents, regulated by a market agent. Each consumer agent passes a bid curve to the market agent, who calculates an optimum for the producer agent. The regulating market agent can be an MPC so that it acts as a higher-level regulator.

District heating networks with many prosumers and a bidirectional energy flow between participants, also called smart district heating networks, have been a recent subject of study in many research papers. The focus is, however, on design optimization and evaluating the implications of different hydraulic layouts and system configurations. Wirtz et al. [13] presented a novel design methodology based on linear programming for designing bidirectional low-temperature networks. The mathematical model determines the optimal selection and sizing of all energy conversion units in buildings and energy hubs while minimizing total annualized costs. Only a few papers address the difficulties arising from the decentralized feed-in and bidirectional heat flow. The effects of decentralized feed-in to the district heating grid have been studied in a simulation study with decentralized solar collectors by Brand et al. [14]. They concluded that the possible local effects of the feed-in may include lower supply temperature, increased flow velocity, and may change the differential pressure. In another simulation study, Heymann et al. found that the flow direction within the district heating grid can change due to different feed-in points, resulting in a supply frontier without flow. Consequently, the temperature drops, leading to stronger thermal stress of the pipes [15].

An overview of different optimization approaches applied to district heating networks is presented in [16,17]. In summary, most optimization problems in district heating networks concern either the design stage or operation with a single or a small number of heat generators without heat flow in arbitrary directions. Our approach, which consists of solving the problem directly as an MINLP in real-time by using existing integer approximation techniques, is not mentioned in this review.

Instead of solving the MINLP directly, it is often possible to transform the nonlinear equations into linear ones by introducing auxiliary variables. For instance, the McCormick relaxation or other (convex) transformation methods [18–20] can be applied to obtain linear approximations. Other approaches may avoid nonlinearities by application of piece-wise linear approximations [21]. However, all these reformulation methods come at the price of a largely increased number of optimization variables and constraints, which may offset the advantages of linear functions [21]. Furthermore, applying such techniques to linearize the original MINLP may not always be applicable. It is typically not favorable in an optimal control setting to apply a general MINLP solver [22]. Instead, tailored solution methods such as the combinatorial integer approximation (CIA) technique have been presented in [22,23] that facilitate an approximate solution of the original MINLP to obtain a fast, however, possibly suboptimal solution to the problem. This approach has been applied in [24,25] to a building cooling system with solar thermal energy production with discrete characteristics in the cooling production plant.

1.3. Contributions

This work presents an initial feasibility study to manage cooperative, bidirectional heat transfer between buildings in a district heating network with decentralized heat production and storage. We propose a simplified, control-oriented model of the prosumer-based heating network, taking into account nonlinearities from the dependency of the amount of transferred heat on storage temperatures but neglecting heat transfer losses and delays within the network. For larger networks, we propose a two-level approach. First, the optimal times for central heat provision are calculated or fixed, followed by the computation of one-at-a-time bidirectional heat transfer between buildings within a neighborhood building cluster. The resulting MIOCP is solved as an MINLP formulation with a combinatorial integer approximation method. The central control by MPC of the bidirectional heat transfer from buildings with heat surplus to buildings with heat demand is a new problem formulation. It results in a nonlinear optimization problem with a large number of discrete decision variables representing the possible heat transfer options.

The method is applied to control an existing district heating network with 37 buildings equipped with building-level solar thermal collectors. The network is divided into four clusters, and heat transfer operations are calculated independently for each cluster. The example demonstrates the potential of the bidirectional heat transfer to support network self-supply with locally generated renewable energy sources. Nevertheless, our work also reveals an important finding: despite numerous simplifications and the consideration of relatively small clusters, the solution of the MINLP problem remains notably challenging in real-world scenarios. This work extends the conference contributions [26,27] in which this type of interconnected community network has been addressed first and optimized in a small case study with up to six buildings. In [26], this problem was solved with a heuristic integer rounding procedure. Kollmar et al. [27] compared different approaches based on CIA and reformulation to a MILP.

1.4. Structure of the paper

The paper is organized as follows: Section 2 introduces the heating network model with bidirectional heat transfer and develops the formulation of the cooperative bidirectional heat transfer between buildings. In Section 3, we explain the MPC formulation, followed by descriptions of the solution methods applied to the optimization problem. The results of the new MPC approach, when applied to an existing district heating network, are presented in Section 4.

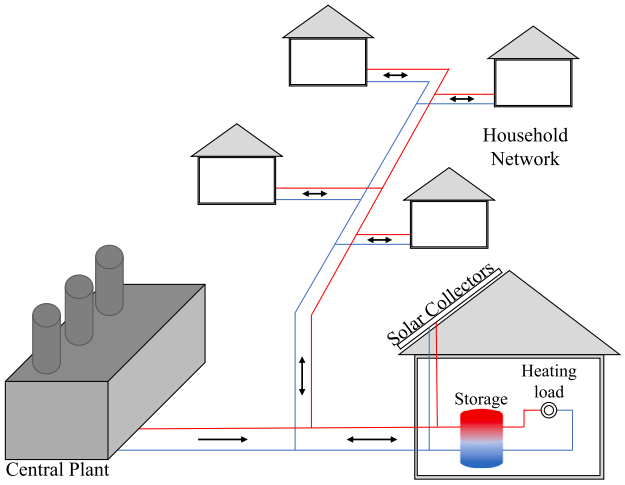

Fig. 1. Sketch of the district heating network with buildings as heat consumers.

2. Model of a prosumer-based district heating network

2.1. System overview

The district heating network considered in this work consists of single and multi-family houses and a few non-residential buildings, each with distributed heat generation and storage facilities. Each building consumes heat for space heating and domestic hot water demand. The heat demand profiles of the buildings vary significantly due to the heterogeneous user behaviors and differing building sizes. Decentralized heat production is influenced by factors such as the size of the thermal collector and the return temperature from the building's storage tank. The collector size is determined by the building's dimensions and the number of housing units it accommodates. It is important to acknowledge that not all solar thermal collectors perform equally, and occasional failures in some plants are not uncommon. Consequently, the solar yield of each individual plant also differs across buildings. Each building is equipped with a storage tank of an appropriate capacity, capable of storing heat for a few hours. The total capacity of the storage tanks in the network exceeds that of the pipe network. These tanks contribute to the overall self-sufficiency of the heating network by offering flexibility through storage options. The water heated by the solar collector system is directed into the storage tank, where it can be used for immediate self-consumption, used to charge the storage tank, or supplied to another building within the network. The central heating plant is only activated when the solar collectors fail to produce sufficient heat to meet the heating requirements. This occurs when the temperature of a specific sensor in one of the storage tanks falls below a predefined threshold. In such cases, heat is transferred from the central heating plant to the storage tank of the respective building. For a visual representation of the network discussed in this paper, please refer to Fig. 1.

A pipe network interconnects the buildings through separate pipes for hot water flow and cold return water flow. This pipe network is further linked to the central heating plant. The residential heating network can be operated in two modes. In the cooperative household heating network modes (HHN), buildings transfer heat to other buildings. In the district heating network mode (DHN), the central plant is in operation.

2.2. Model description

In the following, the model for optimizing the heating network operation consisting of M buildings is described in detail. The scheme of the building installations is shown in Fig. 2. We assume that all

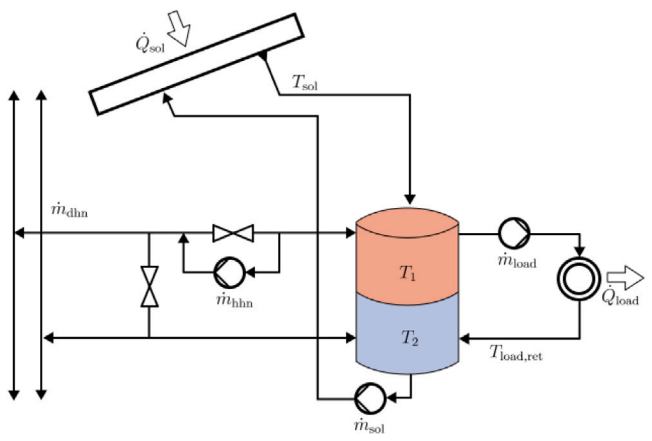

Fig. 2. Scheme of the building installations with storage tank connected to STC and house connection station. Buildings can receive and transfer heat via the district heating pipes.

buildings are equipped in the same way and differ only in the heat consumption profile $\dot{Q}_{\text{load}}$, solar collector sizes, and storage tank sizes.

For each building i, the heat demand $\dot{Q}_{\text{load},i}$ is provided as a forecast. Together with the constant return temperature $T_{\text{load,ret}}$ of the hot water system, it gives the mass flow rate $\dot{m}_{\text{load},i}$:

$$\dot{m}_{\text{load},i}(t) = \frac{\dot{Q}_{\text{load},i}(t)}{c_{\text{w}}(T_{i,1}(t) - T_{\text{load,ret}})} \tag{1}$$

where c_{w} denotes the specific heat capacity of water and $T_{i,1}$ represents the temperature in the top of the storage tank. To cover the heat demand, $T_{i,1}$ must not fall below a minimum temperature $T_{\text{dhw,set}}$.

To simplify the model dynamics and number of variables, the solar thermal yield is calculated externally and enters the model as a parameter forecast. The STC model returning the mass flow rate $\dot{m}_{\text{sol},i}$ and the collector outlet temperature $T_{\text{sol},i}$ given the forecast of solar yield $\dot{Q}_{\text{sol},i}$ is described in Section 2.3.

The water storage tank is modeled as a stratified storage with two storage layers. $T_{i,1}$ and $T_{i,2}$ denote the upper layer and lower layer storage temperature, respectively, and m_i denotes the water mass of a storage layer. The temporal development of the storage temperatures results from the energy balances:

$$\frac{\mathrm{d}T_{i,1}(t)}{\mathrm{d}t} = -U_{\text{eff}} A_{\text{s}} \left(T_{i,1}(t) - T_{\text{amb}}(t)\right) \tag{2a}$$
$$- \frac{\lambda_{\text{eff}}}{h} A_{\text{c}} \left(T_{i,1}(t) - T_{i,2}(t)\right) \tag{2b}$$
$$- \frac{1}{m_i c_{\text{w}}} \Big(\dot{m}_{\text{load},i}(t) c_{\text{w}} \left(T_{i,1}(t) - T_{i,2}(t)\right) \tag{2c}$$
$$+ \dot{m}_{\text{sol},i}(t) c_{\text{w}} \left(T_{\text{sol},i}(t) - T_{i,1}(t)\right) \tag{2d}$$
$$+ \dot{m}_{\text{dhn},i}(t) c_{\text{w}} \left(T_{\text{dhn,set}} - T_{i,1}(t)\right) \tag{2e}$$
$$- \sum_{\substack{1 \le j \le M \\ j \ne i}} b_{\text{hhn},i,j}(t) \dot{m}_{\text{hhn}} c_{\text{w}} \left(T_{i,1}(t) - T_{i,2}(t)\right) \tag{2f}$$
$$+ \sum_{\substack{1 \le j \le M \\ j \ne i}} b_{\text{hhn},j,i}(t) \dot{m}_{\text{hhn}} c_{\text{w}} \left(T_{j,1}(t) - T_{i,1}(t)\right) \Big), \tag{2g}$$

$$\frac{\mathrm{d}T_{i,2}(t)}{\mathrm{d}t} = -U_{\text{eff}} A_{\text{s}} \left(T_{i,2}(t) - T_{\text{amb}}(t)\right) \tag{3a}$$
$$+ \frac{\lambda_{\text{eff}}}{h} A_{\text{c}} \left(T_{i,1}(t) - T_{i,2}(t)\right) \tag{3b}$$
$$- \frac{1}{m_i c_{\text{w}}} \Big(\dot{m}_{\text{load},i}(t) c_{\text{w}} \left(T_{i,2}(t) - T_{\text{load,ret}}\right) \tag{3c}$$
$$+ \dot{m}_{\text{sol},i} c_{\text{w}} \left(T_{i,1}(t) - T_{i,2}(t)\right) \tag{3d}$$
$$+ \dot{m}_{\text{dhn},i}(t) c_{\text{w}} \left(T_{i,1}(t) - T_{i,2}(t)\right) \tag{3e}$$
$$- \sum_{\substack{1 \le j \le M \\ j \ne i}} b_{\text{hhn},i,j}(t) \dot{m}_{\text{hhn}} c_{\text{w}} \left(T_{i,2}(t) - T_{j,2}(t)\right) \tag{3f}$$
$$+ \sum_{\substack{1 \le j \le M \\ j \ne i}} b_{\text{hhn},j,i}(t) \dot{m}_{\text{hhn}} c_{\text{w}} \left(T_{i,1}(t) - T_{i,2}(t)\right) \Big), \tag{3g}$$

for $i = 1, \dots, M$.

Table 1
Notation of state and control variables for a building i, $1 \le i \le M$.

Name	Type	Description	Bounds
$T_{i,1}$	State	Temperature lower storage layer	$[0, 100\ °\text{C}]$
$T_{i,2}$	State	Temperature upper storage layer	$[0, 100\ °\text{C}]$
$\dot{m}_{\text{dhn},i}$	Control	Mass flow central heat	$[0, \dot{m}_{\text{dhn,max}}]$
$b_{\text{hhn},i,j}$	Control	Indicator variable building heat flow $i \to j$, $i \ne j$	$\{0, 1\}$

Table 2
Notation of parameter forecasts.

Parameter	Description
$\dot{Q}_{\text{load}}$	DHW and heating load
$\dot{Q}_{\text{sol}}$	Produced solar thermal heat

Table 3
Notation of constants for the heat storage. Dimensions of the storage tank depend on specific storage size.

Symbol	Description	Value
c_{w}	Specific heat capacity water	4190 J/(kg K)
U_{eff}	Heat transfer coefficient of the walls	0.5 W/(m^2 K)
λ_{eff}	Effective vertical heat conductivity	1 W/(m K)
A_{s}	Surface area of storage layer	–
A_{c}	Cross section area of storage layer	–
h	Height of storage layer	–
T_{amb}	Ambient temperature of storage tank	20 °C

Table 4
Notation of constants for the heating network.

Symbol	Description
$\dot{m}_{\text{dhn,max}}$	Maximum central heat generation mass flow
$\dot{m}_{\text{hhn}}$	Building heat exchange mass flow
$T_{\text{dhn,set}}$	Supply temperature of central heating plant
$T_{\text{load,set}}$	Set-point supply temperature for building load
$T_{\text{load,ret}}$	Return temperature building load
$\dot{Q}_{\text{hhn,min}}$	Minimum heat exchange flow

A summary of the notations for states, controls, parameter forecasts, and constants is provided in Tables 1, 2, 3, and 4. The transmission losses to the exterior (2a) and (3a) and heat conduction between the two layers (2b) and (3b) are considered. This model is a simplified version adapted from [28], where the discrete switching variable that distinguishes between the dominance of cooling load mass flow and heating supply mass flow is relaxed, and all heat flows are considered simultaneously.

The incoming heat flows from the central heating plant, another building, or the STC enter the first layer. The outgoing heat flow's cold return water enters the bottom layer. Both hot and cold water flows lead to bidirectional, vertical heat flows inside the storage tank and a mixing of the temperatures of the two layers. The cooling heat flows resulting from the hot water draw are represented by (2c) and (3c). The heat flows resulting from the generated solar thermal heat are represented by (2d) and (3d).

Eq. (2e) refers to the heat obtained from the central plant. The continuous decision variables $\dot{m}_{\text{dhn},i}$ indicate how much heat must be transferred from the central producer to building i. We assume the central plant provides heat at a constant temperature $T_{\text{dhn,set}}$. Due to the mixing of the storage tank, the temperature of the lower layer changes according to (3e).

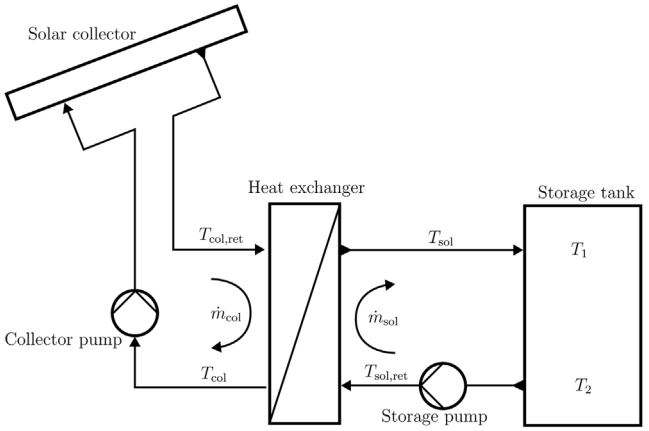

Fig. 3. Hydraulic scheme of STC (adapted from [29]) consisting of collector-heat exchanger cycle (left) and heat exchanger-storage cycle (right). An internal rule-based controller regulates the pumps.

In addition to the central heat provider, buildings have the option of meeting their heating demands through individual heat supply from other buildings. The binary variable $b_{\text{hhn},i,j}$ determines whether there is a heat flow from building i to building j at a given time ($b_{\text{hhn},i,j}(t) = 1$). When this condition is met, hot water flows from the upper layer of storage i through the pipes of the district heating network and enters the upper layer of storage j. Simultaneously, the cold return water flows from the lower layer of storage j through the district heating network pipes and enters the lower layer of storage i. To calculate the total return flows associated with heat transfers from building i to one or multiple buildings j, the individual flows are summed up, as shown in Eqs. (2f) and (3f). The same principle applies to building i receiving heat from one or multiple other buildings j, as illustrated in Eqs. (2g) and (3g).

The heat flows from the central heating plant are defined as

$$\dot{Q}_{\text{dhn},i}(t) = \dot{m}_{\text{dhn},i}(t) c_{\text{w}} \left(T_{\text{dhn,set}} - T_{i,2}(t)\right) \geq 0 \quad \forall i. \tag{4}$$

The heat flows from building i to building j are defined as

$$\dot{Q}_{\text{hhn},i,j}(t) = b_{\text{hhn},i,j}(t) \dot{m}_{\text{hhn}} c_{\text{w}} \left(T_{i,1}(t) - T_{j,2}(t)\right) \geq 0 \quad \forall i, j, i \neq j. \tag{5}$$

Note that, according to this formulation, only one of the two opposing heat flows $\dot{Q}\text{hhn}, i, j$ and $\dot{Q}\text{hhn}, j, i$ can be positive at most.

Section 2.4 provides an explanation of the hydraulic realization of heat transfer. The mass flow rates $\dot{m}_{\text{hhn}}$ are regulated to a fixed value by the decentral pumps at the buildings' substations, allowing us to consider them as constant. On the other hand, the mass flows from the central plant, $\dot{m}_{\text{dhn}}$, cannot be regulated by the MPC controller but are instead controlled by the central DHN heating plant's controller. We treat them as optimization variables to compute a feasible solution with minimum central heat supply. The differential equations (2) and (3) are bilinear in the states T and controls, incorporating binary control variables $b_{\text{hhn},i,j}$, $1 \leq i, j \leq M$, $i \neq j$ for building heat transfer, as well as continuous control variables $\dot{m}_{\text{dhn},i}$, $1 \leq i \leq M$ for the central heat supply.

2.3. Solar thermal collector model

Solar thermal collectors (STC) absorb the radiation of sunlight, which leads to an increase in the internal energy of the heat transfer fluid. The model of the STC system consists of two parts: the model of the STC and the model of the heat distribution system connecting the collector to the storage tank.

The hydraulic scheme of STC is given in Fig. 3. The collector system is coupled to the hot water tank via a heat exchanger. There

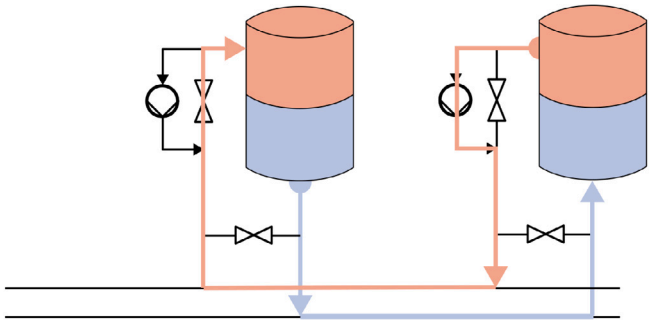

Fig. 4. Hydraulic realization of heat transfer from upper storage tank to lower storage tank containing the decentral pumps, bypass valves (the two left valves) and control valves (the two valves on the right side).

are two hydraulic circuits: the collector circuit connected to the STC and the solar circuit connected to the hot water tank. The mass flow rates in both circuits are regulated by pumps controlled by low-level controllers. The pumps adjust the mass flows such that the temperature in the collector cycle does not become too high and the produced thermal heat is maximized. The exact behavior of the collector and the solar cycles are difficult to model. Instead, we make a simplifying assumption and assume that the mass flows are adjusted such that the water temperature entering the storage tank exceeds the storage tank temperature by $\Delta T = 5$ K. The mass flow of the solar heat entering the storage tank is then computed as follows:

$$\dot{m}_{\text{sol}}(t) = \frac{\dot{Q}_{\text{sol}}(t)}{c_{\text{w}}(T_{\text{sol}}(t) - T_{i,2}(t))} = \frac{\dot{Q}_{\text{sol}}(t)}{c_{\text{w}}(T_{i,1}(t) + \Delta T - T_{i,2}(t))}. \tag{6}$$

The collector outlet temperature $T_{\text{sol},i}$ is computed as follows:

$$T_{\text{sol},i}(t) = T_{i,2}(t) + \frac{\dot{Q}_{\text{sol},i}(t)}{c_{\text{w}} \dot{m}_{\text{sol},i}(t)} \tag{7}$$

where the bottom storage temperature $T_{i,2}$ equals the solar collector inlet temperature. In this context, we make the assumption that the amount of generated heat $\dot{Q}_{\text{sol}}$ is given as an externally computed forecast. This approach helps reduce the number of optimization variables and system equations, thereby facilitating scalability.

2.4. Model of the bidirectional heat transfer between buildings

Fig. 4 illustrates the hydraulic realization of heat transfer between buildings. As explained in Section 2.1, the network operates in two modes, namely HHN (household heating network) and DHN (district heating network). The two modes cannot be active simultaneously since they utilize the same pipes for heat transfer. In the HHN mode, buildings collaborate to exchange heat while the central heat provider's heat distribution is disabled, and vice versa. It is important to note that a building cannot supply heat to the grid unless another building receives it. This new concept, developed in [2], incorporates additional decentral pumps and heat meters at the buildings' substations to facilitate bidirectional heat transfer. In the HHN mode, the MPC controller assumes control and governs the operation of the decentralized pumps and valves. The heat transfer from a building i with surplus heat to a building j with a heat demand is executed as follows, as described in [2]: The decentralized pump in building i propels the heat through the flow of the heating network towards building j. Once the heat meter in the receiving building j detects the arrival of excess heat, the bypass valve is closed, and the control valve is opened, allowing the heat to be pumped into building j's storage tank. The process is terminated when the storage tank of building j has been adequately charged or if building i no longer has surplus heat available in its storage tank.

In DHN mode, the standard district heating controller controlling the central pump of the central heat producer is in charge and supplies

heat to the buildings with a storage temperature lower than a threshold. This mode is not governed by the MPC controller.

The primary objective of the MPC algorithm is to generate a schedule for the building heat transfer operations. Consequently, the thermal network model is significantly simplified by making the following assumptions:

- No consideration is given to time delays caused by heat propagation in the network.
- Heat losses within the network are disregarded.
- Thermal network's inertia is neglected.

The hydraulic topology and characteristics of the heating network introduce constraints on heat transfer. The rules are summarized as follows:

- HHN and DHN modes are not active at the same time.
- If DHN mode is active, one or more buildings can receive heat from the central plant.
- A building cannot send and receive heat at the same time.
- A building can only send heat to another house if it is not too far away and the connecting pipes have similar dimensions.
- Minimum amount of heat transferred between buildings must be larger than $\dot{Q}_{\text{hhn,min}}$.

Due to the slow response of the heating network to changes, a constraint is imposed on the minimum heat exchange quantity. For the heat flow between buildings, we impose a minimum heat flow constraint

$$\dot{Q}_{\text{hhn},i,j}(t) \geq b_{\text{hhn},i,j}(t)\dot{Q}_{\text{hhn,min}} \quad \forall i, j, i \neq j. \tag{8}$$

In DHN mode, several houses can receive heat from the central heating plant at each time point. How many and which operations can occur simultaneously in the HHN mode depends on the constraint formulation. The hydraulic configuration allows for multiple simultaneous heat transfer operations between buildings. However, to avoid uncontrolled mixing of heat flows, changes in flow direction within the pipes, and subsequent uncontrolled heat losses, additional constraints are enforced on the total number and type of simultaneous operations in HHN mode. For larger or branched networks, network partitioning into clusters is practical. To this aim, we limit the simultaneous operations to only one transfer between two buildings at any given time in each cluster. This option is straightforward to implement hydraulically and effectively mitigates the risks of mixing and heat losses. Larger networks can be divided into separate clusters, where only buildings within the same cluster can exchange heat with each other. The rationale behind this is that when located in different parts of the heating network, multiple heat transfer operations can occur, as shown in Fig. 5. Conversely, if the central heat provider is activated in one cluster (DHN mode), all building clusters will also be in DHN mode.

Let K be the number of disjoint clusters and $I_k \subseteq \{1, \dots, M\}$ be the indices of the cluster k with $\cup_{1\leq k\leq K} I_k = \{1, \dots, M\}$. Using the binary decision variables $b_{\text{hhn},i,j}$ for the heat flow from building i to j, the heat transfer constraints are formulated as follows:

$$\sum_{\substack{i,j\in I_k \\ i\neq j}} b_{\text{hhn},i,j}(t) \leq 1 \quad \text{for } 1 \leq k \leq K. \tag{9}$$

In mathematical terms, the constraints form logical special ordered set of type 1 constraints (SOS1). They define a set of variables, at most one of which can take a non-zero value, all others being at 0. These constraints commonly arise in problems where at most one option can be chosen from a given set of possibilities. The special structure of these constraints can be exploited by the mixed-integer optimization algorithm.

3. Model predictive control of the prosumer-based district heating network

MPC requires predictions of future disturbances, e.g., weather, heat demand, availability of renewable energy sources, and electricity grid state, and repeated system state measurements. Using predictions in the optimization routine serves to anticipate the building's energy demand and control its thermal behavior based on the defined target; the measurements keep the model error low. The basic principle of MPC is to solve a time-dependent optimization problem, called optimal control problem (OCP), at each sampling interval using the new measurements of the system state and forecasts. The objective of this study is to develop an initial methodology for determining an optimized control strategy for bidirectional heat transfer among buildings in the network. To simplify the analysis, we make the following assumptions:

- We do not consider any model-plant mismatch.
- We assume that accurate forecasts of building energy demand and solar thermal energy yield are readily available.

It should be noted that these assumptions prevent us from drawing any conclusions about the actual performance of MPC in real-world scenarios.

3.1. Optimal control formulation

Let $x \in \mathbb{R}^{n_x}$ be the differential states, $u \in \mathbb{R}^{n_u}$ the continuous controls, $b \in \{0,1\}^{n_b}$ the binary controls, $p \in \mathbb{R}^{n_p}$ the time-varying parameters, and $s \in \mathbb{R}^{n_s}$ slack variables.

The differential state vector is given by

$$x(t) = (T_{1,1}(t), T_{1,2}(t), \dots, T_{M,1}(t), T_{M,2}(t))^\top.$$

The number of differential states for the residential heating network depends on the number of buildings M. The number of modeled layers in the storage tank is assumed to be 2, thus, the model contains $n_x = 2M$ states.

The binary control vector

$$b(t) = (b_{\text{dhn,on}}(t), b_{\text{hhn}}(t))^\top$$

is composed of $b_{\text{dhn,on}}$, which determines if DHN mode is activated, and the vector

$$b_{\text{hhn}}(t) = (\{b_{\text{hhn},i,j}(t)\}_{1\leq i,j\leq M, i\neq j})^\top$$

determining the heat flows between any two buildings. The continuous control vector $u(t)$ determines the mass flows rates from the central plant:

$$u(t) = (\dot{m}_{\text{dhn},1}(t), \dots, \dot{m}_{\text{dhn},M}(t))^\top.$$

The amount of decision variables depends on the number of buildings and equals $n_u = M$ and $n_b = M(M-1)+1$.

For instance, for $M = 3$ buildings, we have a total of $n_x = 6$ differential states, $n_b = 7$ binary controls and $n_u = 3$ continuous controls.

The number of time-varying parameters is $n_p = 2M$, namely

$$p(t) = [\dot{Q}_{\text{load},\{1\dots M\}}(t), \dot{Q}_{\text{sol},\{1\dots M\}}(t)]^\top.$$

The proposed optimal heat transfer control formulation should favor the heat exchange between buildings and coverage via the heat storages over a request for heat from the central plant. In particular, the total duration DHN mode has to be activated should be minimized. That means if different houses require heat from the central heating plant, they should ideally obtain it at the same time. This objective serves to shut off the central heating plant as long as possible and maximize the network self-coverage, avoiding the high network heat distribution losses and maintenance requirements associated with frequent activation of the central heating plant. According to the problem definition, the central plant should be active only when the heat demand of the network exceeds the total amount of stored heat.

The optimal bidirectional heat transfer operations for each building cluster in HHN mode are determined by solving the following OCP

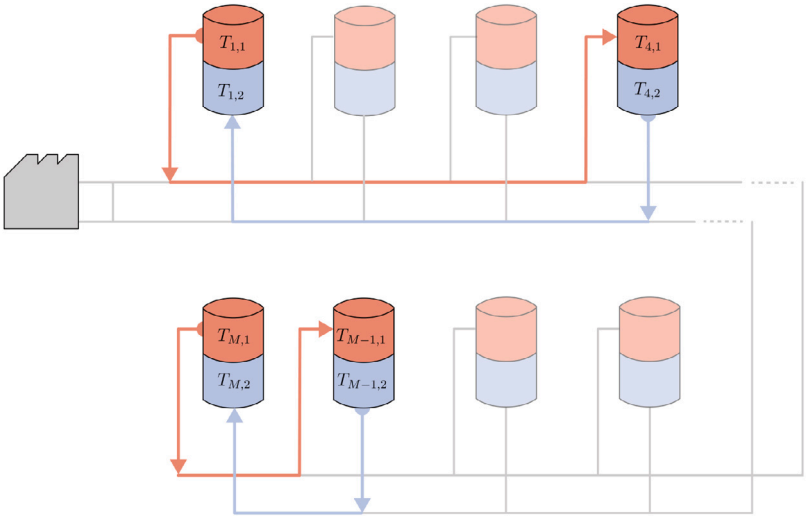

Fig. 5. Example of disjoint parallel heat transfer operations in the network: building 1 transfers heat to buildings 4, building M transfers heat to building $M-1$.

for each cluster k, $k = 1, \dots, K$. As defined in the previous section, $I_k \subseteq \{1, \dots, M\}$ are the indices of the cluster k.

$$\min_{x,u,b_{\text{hhn},s}} \quad \int_{t_0}^{t_f} \sum_{i \in I_k} b_{\text{dhn,on}}(t)\dot{Q}_{\text{dhn},i}(t) + c_s^\top s(t)\mathrm{d}t \tag{10a}$$

$$\text{s.t.} \quad \text{for } t \in [t_0, t_f]:$$

$$\dot{x}(t) = f(x(t), b(t), u(t), p(t)), \tag{10b}$$

$$x(t_0) = x_0, \tag{10c}$$

$$\sum_{i,j \in I_k, i \neq j} b_{\text{hhn},i,j}(t) \leq 1, \tag{10d}$$

$$\dot{Q}_{\text{hhn},i,j}(t) \geq b_{\text{hhn},i,j}(t)\dot{Q}_{\text{hhn,min}} \quad \forall i, j \in I_k, i \neq j, \tag{10e}$$

$$T_{\text{lb}} - s(t) \leq x(t) \leq T_{\text{ub}} + s(t), \tag{10f}$$

$$s(t) \geq 0, \tag{10g}$$

$$u(t)(1 - b_{\text{dhn,on}}(t)) = 0, \tag{10h}$$

$$b_{\text{hhn}}(t)b_{\text{dhn,on}}(t) = 0, \tag{10i}$$

$$b(t) \in \{0, 1\}^{n_b}, \tag{10j}$$

$$u(t) \in [0, u_{\text{ub}}]^{n_u}. \tag{10k}$$

For a small network, a single cluster spanning the entire network is sufficient. The on-times of the DHN mode are pre-determined as detailed in the subsequent section.

The parameters, bounds and constants are introduced in Section 2.2. The objective minimizes the sum of heat supply from the central district heating plant as defined in Eq. (4) and the comfort deviation defined as storage temperature constraint Eq. (10f). A small deviation of the storage temperature constraint is allowed, thus giving the optimizer more degrees of freedom in finding a good solution. Slack variables $s(t) \in \mathbb{R}^{n_s}$, $n_s = n_x$, are introduced for the relaxation of the temperature constraint. The minimization of comfort deviation is achieved by minimizing the slack variables weighted by a corresponding cost vector $c_s \in \mathbb{R}^{n_s}$.

The temperature evolution gives the system dynamics in the storage tank with Eqs. (2) and (3). Eq. (10c) determines the initial state. Eqs. (10d) and (10e) are conditional constraints depending on the value of the binary variables. They define the conditions on the district heating and building heat transfer operations and the minimum sizes of the heat flows whenever they are not zero. Bounds on the temperature states, augmented by slack variables, are given by (10f). They include, in particular, the condition that the upper storage layer temperature must always be higher than $T_{\text{load,set}}$, the set-point temperature for satisfying the heating loads. Eq. (10g) restricts the value of the slack variables to be positive, (10h) and (10i) are the operating time constraints for DHN and HHN mode. Eqs. (10j) and (10k) represents the bounds on the decision variables.

3.2. Determination of central heat production times

When partitioning the network into clusters, we face the challenge of determining consistent central heat provision times $b_{\text{dhn,on}}$, during which the DHN mode is activated across all clusters.

We propose a formulation with pre-defined time slots determined by a higher-level optimization, such as times with favorable market conditions for turning on the central heating plant. Following the problem description and the listed requirements, the optimization routine needs to determine the optimal times for central operation (DHN mode is active) as well as the bidirectional heat transfer operations in HHN mode (DHN mode is inactive). The problem can be formulated as a bi-level optimization problem. The higher-level optimization (11) allocates the optimal DHN times depending on external conditions such as given energy prices c_{grid}. The objective is to select the times with minimum energy prices for the necessary central heating plant operation. The lower-level optimization (10), abbreviated for each cluster k, $k = 1, \dots, K$ as OCP(k), then assigns the heat transfer operations for each building cluster.

$$\min_{b_{\text{dhn,on}}} \quad \int_{t_0}^{t_f} c_{\text{grid}}(t)b_{\text{dhn,on}}(t)\mathrm{d}t \tag{11a}$$

$$\text{s.t.} \quad \text{OCP}(k) \qquad \forall k \in 1, \dots, K \tag{11b}$$

$$b_{\text{dhn,on}}(t) \in \{0, 1\} \quad \forall\, t \in [t_0, t_f]. \tag{11c}$$

Bi-level optimization problems are generally hard to solve, therefore, we propose a two-step procedure. First, the optimal times for DHN operation for the whole network are determined by solving a simple integer linear optimization problem, defined in (12), in which we impose a duration of T hours for the DHN operation. To this aim, we discretize the time horizon $[t_0, t_f]$ in N equidistant time steps on which $b_{\text{dhn,on}}$ is constant:

$$b_{\text{dhn,on}}(t) = b_{\text{dhn,on},l} \quad \text{for } t \in [t_l, t_{l+1}],\ l = 0, \dots, N-1.$$

The energy cost vector c_{grid} is discretized similarly.

$$\min_{b_{\text{dhn,on},0}, \dots, b_{\text{dhn,on},N-1}} \quad \sum_{0 \leq l \leq N-1} c_{\text{grid},l} b_{\text{dhn,on},l} \tag{12a}$$

$$\text{s.t.} \quad \sum_{0 \leq l \leq N-1} b_{\text{dhn,on},l} = T, \tag{12b}$$

$$b_{\text{dhn,on},0}, \cdots, b_{\text{dhn,on},N-1} \in \{0,1\}. \tag{12c}$$

In this revised formulation, we separate the upper-level problem from the lower-level problem by considering them as independent problems. As a result, the solution to the upper-level optimization problem becomes independent of the outcomes derived from the lower-level OCP (10), thus obtaining a more tractable formulation.

3.3. Solution methods

The optimized control of the dynamic system in Problem (10) leads to the formulation of a nonlinear mixed-integer optimal control problem (MIOCP). This problem contains an infinite number of values in the time horizon $t \in [t_0, t_f]$ and is discretized using direct collocation [30]. This procedure leads to a large-scale mixed-integer nonlinear program (MINLP). MINLPs are generally much more difficult to solve than MILP. An overview of solution methods and numerical solvers for MINLPs can be found in [31]. General-purpose solution methods often require significant time to solve even moderately sized problems, rendering such solvers unsuitable for use within large-scale real-time control applications. However, tailored approximate solution methods exist that aim at finding a good approximate and fast solution of the original MINLP.

The system dynamics of problem (10) have the special form of a switched bilinear system composed of binary controls multiplied with the differential state. The special form of the system dynamics can be exploited to solve the above optimization problem. We apply the combinatorial integral approximation (CIA) method, an approximation method to solve MINLPs introduced in [23]. The CIA method, described in Algorithm 1, aims to solve discretized MIOCPs by decomposing the original problem into a sequence of three subproblems. First, a relaxed MINLP, where the binary variables are considered to be continuous ($b_{\text{rel}} \in [0,1]^{n_b}$) and thus an ordinary nonlinear program (NLP), denoted as NLP_{rel}, is solved. Using the solution of NLP_{rel}, the so-called CIA problem is solved to yield approximations of the binary controls $b_{\text{bin}} \in \{0,1\}^{n_b}$. In the third step, the NLP is solved again with the approximated binary controls fixed $b = b_{\text{bin}}$, to adjust the remaining optimization variables such as states x, slack variables s and, if applicable, continuous controls u.

Algorithm 1: CIA decomposition algorithm for the solution of MIOCPs

Input : Discretized MIOCP (MINLP), initial guesses for x, u, b, s.
Output: Local optimal variables x^*, u^*, b^*, s^* with objective $F^* = F(x^*, u^*, b^*, s^*)$.

1 Solve relaxed MINLP (NLP_{rel}) $\rightarrow x, u, b_{\text{rel}}, s, F_{\text{rel}}$;
2 Solve CIA problem for $b_{\text{rel}} \rightarrow b_{\text{bin}}$;
3 Solve MINLP with $b = b_{\text{bin}}$ fixed (NLP_{bin}) $\rightarrow x, u, s, F_{\text{bin}}$;
4 **return** $(x^*, u^*, b^*, s^*, F^*) = (x, u, b_{\text{bin}}, s, F_{\text{bin}})$;

The CIA problem (step 2) is an MILP of a special structure that minimizes the maximum integrated difference between the relaxed b_{rel} and binary controls b_{bin}. The CIA problem can be solved, e.g., using standard MILP solvers or tailored Branch-and-Bound (BnB) algorithms [23]. One binary subproblem has to be solved for each cluster in the network.

In practice, the CIA decomposition method shows very good results for mixed-integer problems with SOS1 constraints. It can be extended to include other constraint types such as maximum dwell time constraints and maximum number of switch constraints. Sager et al. [32] and Zeile et al. [33] have presented theoretical findings concerning the integer approximation error. However, these results possess limited practical utility due to the potential presence of considerable constants within the accuracy bounds.

All methods are implemented in Python using the open-source software CasADi [34] for solving optimal control problems, the nonlinear programming solver IPOPT [35] for solving the NLPs and pycombina [36] for the CIA algorithm. Problem (12), which is a simple integer linear problem, can be solved, e.g., with the open-source solver BONMIN [37].

4. Results

This section presents the solution to the optimal control problem for heating networks with distributed heat generation, as described in the previous sections. The method is applied to an existing district heating network with 37 buildings[1] and the results are compared to the measured real operation. A small case study with three buildings is presented first, illustrating the problem formulation and verifying the solution.

The prediction horizon is 24 h, discretized in 1 h steps. Hence, each heat transfer operation has a 1 h duration. The optimized heat transfer trajectories are applied to the system for 24 h.

4.1. The residential heating network

The district heating network located in Freiburg, Germany, connects 37 buildings of different types and sizes, which contain a total of 525 apartments. Each household contains a STC for heat production and a hot water storage. Sizes range from 8.0 m^2 to 179.0 m^2 for the collector area and from 0.8 m^3 to 12.0 m^3 for the storage volume. The total area of the solar collectors is 2200 m^2 and the total storage volume is 160 m^3. In addition to the decentralized heat production, the network is connected to a central heating plant. Fig. 6 shows a photo of the city quarter and Fig. 7 shows the distribution of the thermal collector sizes. The solar thermal collectors, as well as the storage tanks, are operated by the energy provider of the district heating network, which motivates the cooperative, centrally controlled heat transfer between the buildings. If the temperature in the building's storage tanks falls below a certain threshold, see Table 5, a central heat generator is activated and supplies hot water with a temperature of 72 °C.

The amount of the consumed and produced heat in each of the buildings is plotted in Figs. 8 and 9 for the whole year 2020 and the month of June 2020, as an example of a typical summer month. The solar coverage rate is the fraction of heat demand covered by solar thermal heat and defined as $f_{\text{sc}} = 1 - \frac{\dot{Q}_{\text{dhn}}}{\dot{Q}_{\text{load}}}$. If the solar coverage rate is 1, then all heat demand is covered by solar heat. If it is 0, then the complete heat demand must be covered by centrally produced heat. The value can be negative due to additional storage losses that must be covered. The heat demand includes space heating in the cold months, and domestic hot water and hot water circulation throughout the whole year. In some buildings, the solar collectors do not function correctly and produce little or no heat. In June, the actually used solar heat (measured solar thermal coverage in Fig. 8) only covers approximately half of the heat demand. The actually produced solar heat in each building (expected solar thermal coverage in Fig. 8) is higher, and usually covers more than three-quarter of the heat demand. However, the produced heat cannot be fully exploited due to time mismatch between production and demand.

4.2. Small case study

A small case study of three heterogeneous buildings is carried out to illustrate the algorithm. Three buildings are extracted from the large district heating network as shown in Fig. 10. Measurement data for the

[1] As a building we refer to a housing unit that contains a STC and a storage tank. Note that the network consists of 38 buildings, however, only for 37 buildings measurement data was available.

Fig. 6. Prosumer-based district heating network Freiburg-Gutleutmatten, Germany (Copyright: Fraunhofer ISE).

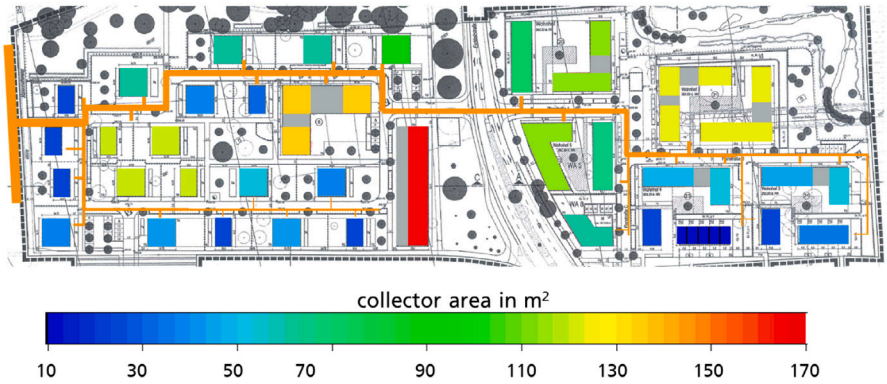

Fig. 7. Layout of city quarter Freiburg-Gutleutmatten with differently sized solar collector areas.

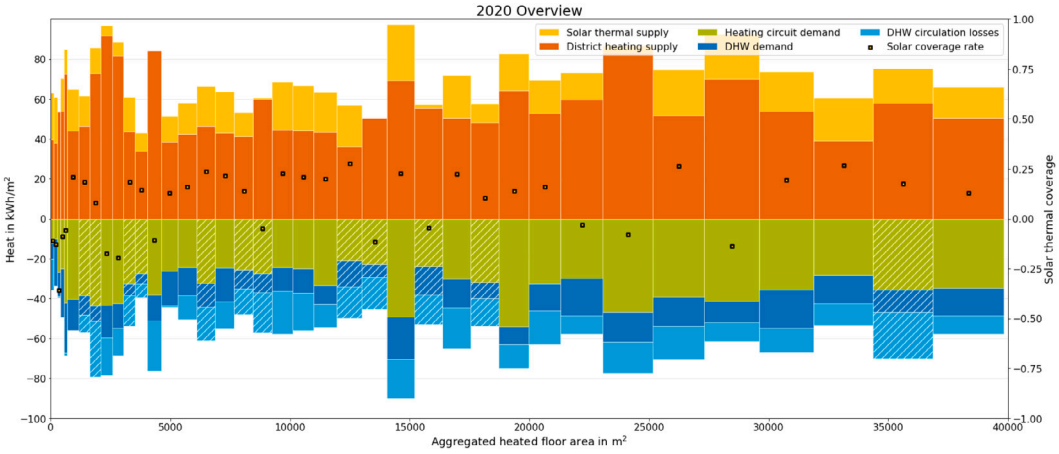

Fig. 8. Heat balance over the year 2020 of the building's heat storage ordered by size of the heated building area (orange: central district heat consumption, yellow: solar heat production, green: space heating, dark blue: domestic hot water, light blue: circulation).

first three days of July 2020 comprising heating load, solar thermal supply, central district heating supply, and storage temperatures was used.

The dimensions of the buildings and the sizes of the solar collectors and storage tanks are summarized in Table 6. The measurement data for the three days is summarized in Table 7 and is illustrated in Fig. 11. All buildings are multi-apartment buildings with 11 up to 37 apartments with an average daily heating demand of approximately 34 up to 190 kWh for domestic hot water production. The average solar heat production is approximately 249 kWh for the first building and 73 kWh for the third building, with an overall lower production on the second day. Building 2 has no solar thermal production due

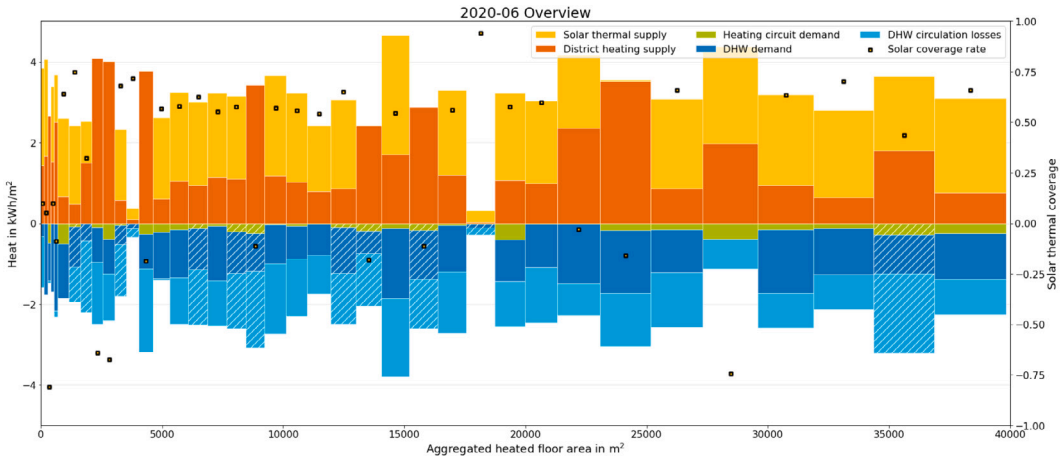

Fig. 9. Heat balance over the month of June 2020 of the building's heat storage. See Fig. 8 for explanations.

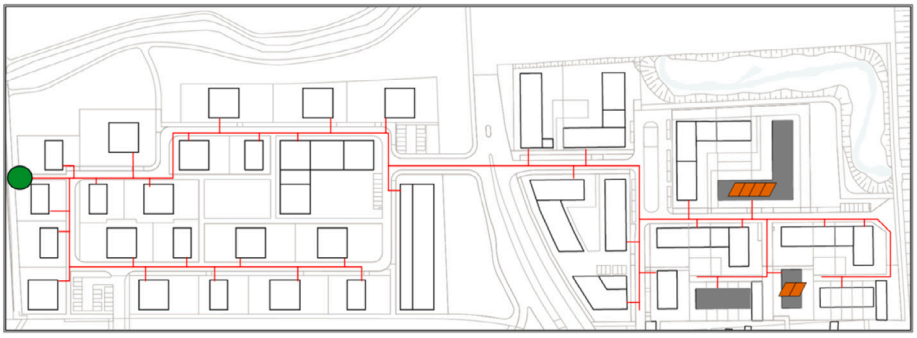

Fig. 10. Case study with three heterogeneous buildings. Large building 1 is on top with a large STC, building 2 has no solar thermal generation and smaller building 3 is located on the bottom right with small solar thermal heat generation.

Table 5
Parameter settings for district heating network.

$T_{load,ret}$	$T_{load,set}$	$T_{dhn,set}$	$\dot{m}_{dhn,max}$	$\dot{m}_{hhn}$	$\dot{Q}_{hhn,min}$
35 °C	58 °C	72 °C	360 l/h	290 l/h	800 W

Table 6
Dimensions of the three example buildings for the first case study.

	No. apartments	A_{heated} [m²]	A_{stc} [m²]	V_{st} [m³]
Building 1	37	2972	168.7	12
Building 2	13	1055	53	4.5
Building 3	11	899	45.8	4.5

to a temporary non-functioning of the solar thermal plant. Over the considered three days in July, the heat demand for all three buildings together is 878.8 kWh, the amount of produced heat is 979.6 kWh and the required heat from the central plant is 255 kWh. Hence, the total amount of produced heat from the solar thermal collectors of building 1 and 3 is sufficient to satisfy the heat demand of the three buildings if the additional heat from building 1 and 3 can be stored and be transferred to building 2. This potential cannot be exploited without a cooperative heat transfer between buildings.

The MPC algorithm can distribute the total generated decentralized solar heat among the three buildings such that no central DHN operation is necessary. Results for three days of operation are given in Table 8. Fig. 12 illustrates the heat transfer operations between the buildings. Buildings 1 and 3 mainly supply heat to building number 2 without any solar heat production. Sometimes, heat transfer between the other buildings takes place in order to balance out heat production

Table 7
Measured heat quantities (heat demand, produced solar heat, heat consumed from the district heating plant) for the small case study for three days for 01/07/2020–03/07/2020.

	Q_{load}^{meas} [kWh]	Q_{sol}^{meas} [kWh]	Q_{dhn}^{meas} [kWh]
Building 1	579.2	746.4	1.0
Building 2	185.3	0	252.3
Building 3	102.1	219.6	1.7
Sum	878.8	979.6	255

Table 8
Heating load and heat supplies resulting from MPC operation for the small case study for 01/07/2020–03/07/2020.

	Q_{dhn} [kWh]	$Q_{hhn,in}$ [kWh]	$Q_{hhn,out}$ [kWh]
Building 1	0	159.4	883
Building 2	0	1060.2	82.5
Building 3	0	128.7	382.9

and demand occurring at distinct time points. In summary, for the three considered days, the necessary heat consumption is reduced by 255 kWh or 100% compared to the real operation. To achieve this, the buildings transfer heat of a total amount of 1348 kWh between each other. If preferred, however, it is possible to prevent extensive heat transfer operations by adding a weighted term to the objective function of the optimization problem. One example solution is given in Fig. 13 with only 698 kWh of transferred heat between the buildings. However, in this solution, a small central heat supply to building 2 is necessary on the second day.

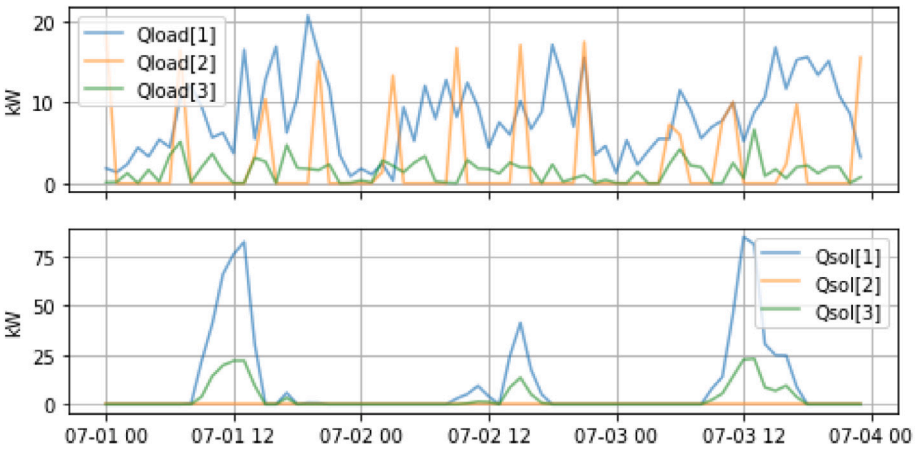

Fig. 11. Heating load (image above) and produced solar thermal heat (image below) for 01/07/2020–03/07/2020.

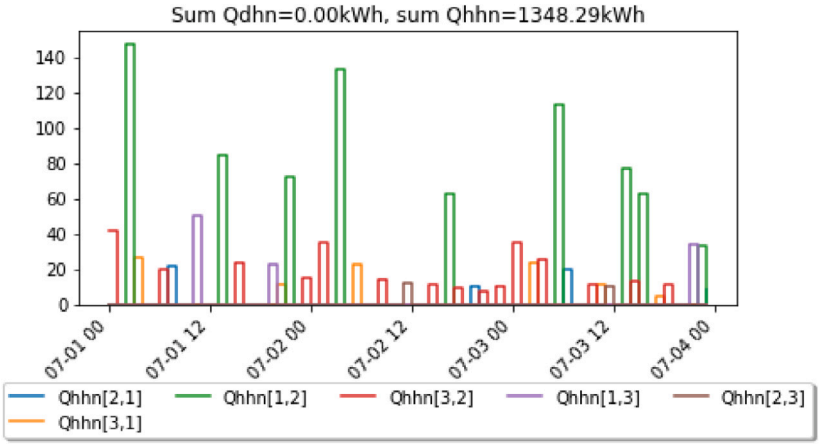

Fig. 12. Cooperative heat transfer resulting from MPC solution for three days in July 2020.

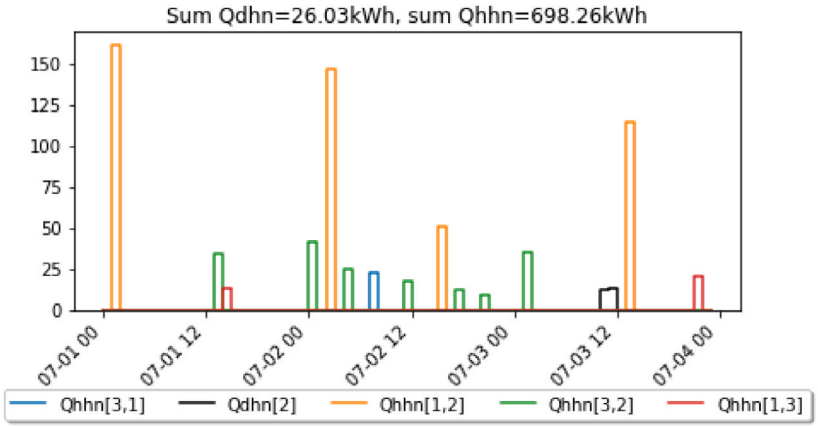

Fig. 13. Cooperative heat transfer resulting from MPC solution with small penalization on heat transfer operations for three days in July 2020.

4.3. Application to residential heating network

The developed methods should be applied to control the central district heating plant operation as well as the decentralized heat distribution between the buildings of the full district heating network. The solution to the optimal control problem for the full district heating networks is computationally more involved. As illustrated in Fig. 14, all buildings are connected via a distributed bus network with several different branches. We divide the network into four partitions that form independent communities for cooperative heat exchange. This partition prevents buildings that are far away from each other and are connected to differently-sized pipes to attempt to transfer heat to each other. The times for the DHN mode operation are pre-determined and set for all partitions equally to two hours at noon and one hour at midnight. For simplicity and to focus on the bidirectional heat transfer operation, we have not directly applied the two-step procedure from Section 3.2 for determining optimal DHN times overall the clusters. For one MPC iteration with a 24 h forecast the problem for each cluster is solved in

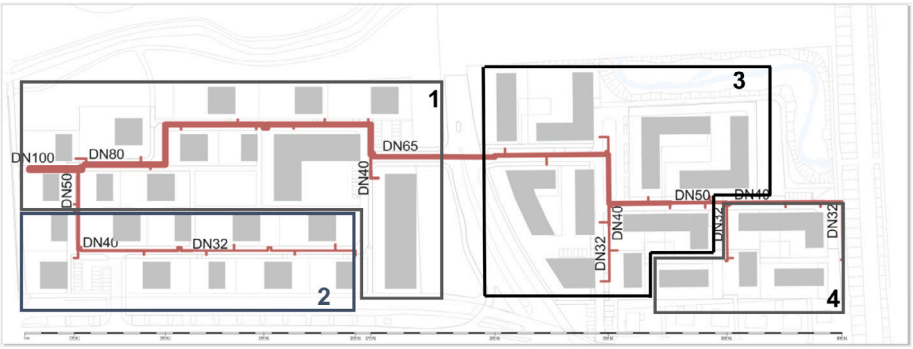

Fig. 14. Partition of the residential district heating network into four independent sections. Note that in the graphic some bigger buildings are composed of smaller buildings with independent solar panels and heat storage.

the range of a few minutes on a laptop equipped with an Intel Core i7-8650U processor, which is below the sampling interval length of 1 h. Runtimes for each cluster are given in Table 9. The predominant portion of the runtime is dedicated to solving the relaxed MINLP, constituting the first step in Algorithm 1. Conversely, the solution of the CIA sub-problem and the MINLP with fixed binary variables only necessitates a few seconds.

The input for the load demand and solar production is the measurement data from June 2020 and given in Table 9. This table also contains the consumed heat from the central heating plant and the resulting heat consumption, the cooperative heat transfer between the buildings computed by the MPC algorithm and the runtimes for one MPC iteration. The number of binary optimization variables for each cluster varies between 72 and 90 for one cluster. Despite dealing with relatively small clusters, the high complexity of the optimization problems (OCPs) is evident, primarily due to the substantial number of binary optimization variables. All four building sections contain one or more buildings with a broken solar collector and little or no solar production - a situation that is not uncommon in practice. In total, the overall solar heat production is lower than the total heat demand. Thus, also the optimized MPC solution must require some operation of the central heating plant to meet the difference between solar heat production and heat demand. In total, the summerly monthly heat demand is approximately 82 MWh while the total solar heat production covers only about 75% or 64 MWh. Even with this large amount of solar heat produced, the actual operation requires a rather large amount of heat in form of 60 MWh from the central heating plant. This unnecessary heat consumption can be avoided with an optimized and predictive MPC algorithm: By using cooperative heat transfer between buildings, only the minimally possible central heating consumption is used if the heat amounts can be matched or stored accordingly. This amount equals approximately the difference between solar production and heat demand: $Q_{\text{dhn}}^{\text{mpc}} \approx Q_{\text{load}}^{\text{meas}} - Q_{\text{sol}}^{\text{meas}}$. Thus the additional heat consumption with an optimized controller covers the remaining 25% of the heating load that cannot be covered by solar heat production. The amount of additionally required heat is approximately 17 MWh and the amount of heat transferred between the buildings in a cooperative operation is approximately 40 MWh.

Table 9
Summary of measured heating load and production (in MWh) and a comparison with the MPC solution for June 2020 for the four considered building clusters. Runtime for one MPC iteration is provided as both the average and maximum values over all MPC iterations.

No. bldgs	$Q_{\text{load}}^{\text{meas}}$	$Q_{\text{sol}}^{\text{meas}}$	$Q_{\text{dhn}}^{\text{meas}}$	$Q_{\text{dhn}}^{\text{mpc}}$	$Q_{\text{hhn}}^{\text{mpc}}$	Runtime
10	30.0	23.4	20.9	5.1	13.5	138 s/16:32 min
8	12.2	6.9	10.9	3.4	6.7	48 s/7:46 min
10	33.8	28.6	22.6	7.9	14.8	116 s/16:25 min
9	5.7	5.3	5.4	1.0	5.4	88 s/10:01 min
Sum	81.7	64.2	59.8	17.4	40.3	

5. Conclusion

Within this work, we investigated the problem of finding optimized strategies for bidirectional heat transfer in district heating networks with decentralized heat production. The network is divided into several neighborhood clusters. To find the optimal strategy for the heat transfer between buildings within each building cluster, we have formulated a mixed-integer nonlinear optimal control problem. It contains binary decision variables that determine the heat exchange between the buildings, therefore resulting in a mixed-integer nonlinear optimization problem that is hard to solve. To ensure real-time solvability, first, the discrete variables are relaxed and treated as continuous. The problem is subsequently solved with a fast gradient-based optimization algorithm in combination with a combinatorial integral approximation strategy to restore the mixed-integer formulation. Next steps involve the integration of a more comprehensive model that accounts for heat losses, transportation delays, and network thermal inertia. Furthermore, we aim to address challenges related to model-plant mismatch and the incorporation of forecasting errors to present a more holistic and realistic solution for prosumer-based DHN management. Additionally, the application of an improved mixed integer approximation technique proposed in [38] seems promising.

The results of the case study with measurement data from an existing medium-sized district heating network show that the optimized strategy can exploit the total amount of heat generated in the whole network, and the central heating provider is only required when the total heat demand exceeds the total heat generation or storages cannot provide heat. In the case study, this leads to a reduction of centrally produced heat by almost 75%.

Finally, this research highlights the gap between theoretical MINLP solutions and their practical application to even medium-sized systems, as indicated by all the simplifying assumptions we had to make. These challenges, particularly in areas like simplifications in the model and optimization routine, emphasize the need for further research. Ultimately, our findings illustrate that applying these concepts in real-world scenarios is a complex and demanding task, underscoring the importance of continued exploration and development in this field.

CRediT authorship contribution statement

Lilli Frison: Writing – review & editing, Writing – original draft, Software, Methodology, Conceptualization. **Manuel Kollmar:** Writing – review & editing, Writing – original draft, Validation. **Axel Oliva:** Writing – review & editing, Supervision, Project administration, Funding acquisition, Conceptualization. **Adrian Bürger:** Writing – review & editing, Supervision, Methodology, Conceptualization. **Moritz Diehl:** Supervision, Funding acquisition, Conceptualization.

Declaration of competing interest

The authors declare the following financial interests/personal relationships which may be considered as potential competing interests: Lilli Frison reports financial support was provided by Federal Ministry for Economics and Climate Action (BMWK). Axel Oliva reports financial support was provided by Federal Ministry for Economics and Climate Action (BMKK).

Data availability

The data that has been used is confidential.

Acknowledgments

L. Frison and A. Oliva acknowledge funding from the German Federal Ministry for Economics and Climate Action (BMWK) via ENWISOL II (03ETS005A+B). M. Diehl acknowledges funding by German Research Foundation (DFG) via Research Unit FOR 2401 and project 424107692 and by the EU via ELO-X 953348.

References

[1] Bundesministerium für Umwelt, Naturschutz und nukleare Sicherheit (BMU). Bundes-klimaschutzgesetz. 2019.
[2] Elci M. Smarte und dezentrale solare fernwärme (Dissertation), Stuttgart Fraunhofer Verlag; 2018.
[3] Ma Y, Borrelli F, Hencey B, Coffey B, Bengea S, Haves P. Model predictive control for the operation of building cooling systems. IEEE Trans Control Syst Technol 2012;20(3):796–803.
[4] Searle G, Fiorentini M, Capozzoli A, Bernardini D, Bemporad A. Model predictive control (MPC) for enhancing building and HVAC system energy efficiency: Problem formulation, applications and opportunities. Energies 2018;11:3.
[5] Madsen H, Sejling K, Søgaard HT, Palsson OP. On flow and supply temperature control in district heating systems. Heat Recovery Syst CHP 1994;14(6):613–20.
[6] Vivian J, Jobard X, Hassine IB, Pietrushka D, Hurink JL. Smart control of a district heating network with high share of low temperature waste heat. In: Proceedings of the 12th conference on sustainable development of energy, water and environmental systems-SDEWES, Dubrovnik, Croatia. 2017, p. 4–8.
[7] Vandermeulen A, Heijde B, Helsen L. Controlling district heating and cooling networks to unlock flexibility: A review. Energy 2018;151:103–15.
[8] Vanhoudt D, Claessens B, Salenbien R, Desmedt J. An active control strategy for district heating networks and the effect of different thermal energy storage configurations. Energy Build 2018;158:1317–27.
[9] Aoun N, Bavière R, Vallée M, Aurousseau A, Sandou G. Modelling and flexible predictive control of buildings space-heating demand in district heating systems. Energy 2019;188.
[10] Verrilli F, Srinivasan S, Gambino G, Canelli M, Himanka M, Del Vecchio C, Sasso M, Glielmo L. Model predictive control-based optimal operations of district heating system with thermal energy storage and flexible loads. IEEE Trans Autom Sci Eng 2017;14(2):547–57.
[11] Wetter M. GenOpt - A generic optimization program. In: Seventh international IBPSA conference. International Building Performance Simulation Association Rio de Janeiro; 2001, p. 601–8.
[12] Bünning F, Wetter M, Fuchs M, Müller D. Bidirectional low temperature district energy systems with agent-based control: Performance comparison and operation optimization. Appl Energy 2017.
[13] Wirtz M, Kivilip L, Remmen P, Müller D. 5Th Generation District Heating: A novel design approach based on mathematical optimization. Appl Energy 2020;260(11415):8. http://dx.doi.org/10.1016/j.apenergy.2019.114158.
[14] Brand L, Calvén A, Englund J, Landersjö H, Lauenburg P. Smart district heating networks – A simulation study of prosumers' impact on technical parameters in distribution networks. Appl Energy 2014;129:39–48. http://dx.doi.org/10.1016/j.apenergy.2014.04.079.
[15] Heymann M, Rühling K, Feldmann C. Integration of solar thermal systems into district heating – DH system simulation. Energy Procedia 2017;116:394–402. http://dx.doi.org/10.1016/j.egypro.2017.05.086.
[16] Olsthoorn D, Haghighat F, Mirzaei P. Integration of storage and renewable energy into district heating systems: A review of modelling and optimization. Sol Energy 2016;136:49–64.
[17] Sameti M, Haghighat F. Optimization approaches in district heating and cooling thermal network. Energy Build 2017;140.
[18] Gabrielli P, Acquilino A, Siri S, Bracco S, Sansavini G, Mazzotti M. Optimization of low-carbon multi-energy systems with seasonal geothermal energy storage: The energy grid of ETH Zurich. Energy Convers Manage 2020;8:10005. http://dx.doi.org/10.1016/j.ecmx.2020.100052.
[19] Harjunkoski I, Pörn R, Westerlund T, Skrifvars H. Different strategies for solving bilinear integer nonlinear programming problems with convex transformations. Comput Chem Eng 1997;21:S487–92. http://dx.doi.org/10.1016/S0098-1354(97)87549-7.
[20] Sherali HD, Adams WP. A reformulation-linearization technique for solving discrete and continuous nonconvex problems. Springer-Verlag; 1999.
[21] Glover F. Improved linear integer programming formulations of nonlinear integer problems. Manage Sci 1975;22:455–60. http://dx.doi.org/10.1287/mnsc.22.4.455.
[22] Sager S. Reformulations and algorithms for the optimization of switching decisions in nonlinear optimal control. J Process Control 2009;19(8):1238–47. http://dx.doi.org/10.1016/j.jprocont.2009.03.008.
[23] Sager S, Jung M, Kirches C. Combinatorial integral approximation. Math Methods Oper Res 2011;73(3):363–80. http://dx.doi.org/10.1007/s00186-011-0355-4.
[24] Bürger A, Zeile C, Altmann-Dieses A, Sager S, Diehl M. Design, implementation and simulation of an MPC algorithm for switched nonlinear systems under combinatorial constraints. J Process Control 2019;81:15–30.
[25] Bürger A, Bull D, Sawant P, Bohlayer M, Klotz A, Beschütz D, Altmann-Dieses A, Braun M, Diehl M. Experimental operation of a solar-driven climate system with thermal energy storages using mixed-integer nonlinear model predictive control. Optim Control Appl Methods 2021;42:1293–319, URL https://doi.org/10.1002/oca.2728.
[26] Frison L, Oliva A, Herkel S. MPC for collaborative heat transfer in a district heating network with distributed renewable energy generation and storage. In: 2021 European control conference (ECC). IEEE; 2021, p. 1669–74.
[27] Kollmar M, Frison L, Bürger A, Oliva A, Altmann-Dieses A, Diehl M. Mixed-integer optimal control of a residential heating network using linear and nonlinear programming techniques. In: 2022 European control conference (ECC). IEEE; 2022, p. 1103–9.
[28] Eicker U. Solar technologies for buildings. Wiley; 2003.
[29] Ferhatbegovic T, Zucker G, Palensky P. Model based predictive control for a solar-thermal system. In: IEEE AFRICON conference, Vol. 10. 2011, p. 1109. http://dx.doi.org/10.1109/AFRCON.2011.6071992.
[30] Rawlings J, Mayne D, Diehl M. Model predictive control: Theory, computation, and design. 2nd ed.. Nob Hill Publishing, LLC; 2020.
[31] Belotti P, Kirches C, Leyffer S, Linderoth J, Luedtke J, Mahajan A. Mixed-integer nonlinear optimization. Acta Numer 2013;22:1–131, 1st Edition.
[32] Sager S, Bock HG, Diehl M. The integer approximation error in mixed-integer optimal control. Math Program 2012;133:1–23.
[33] Zeile C, Robuschi N, Sager S. Mixed-integer optimal control under minimum dwell time constraints. Math Program 2020;188:1–42. http://dx.doi.org/10.1007/s10107-020-01533-x.
[34] Andersson JAE, Gillis J, Horn G, Rawlings JB, Diehl M. CasADi – A software framework for nonlinear optimization and optimal control. Math Program Comput 2019;11(1):1–36. http://dx.doi.org/10.1007/s12532-018-0139-4.
[35] Wächter A, Biegler LT. On the implementation of an interior-point filter line-search algorithm for large-scale nonlinear programming. Math Program 2006;106(1):25–57. http://dx.doi.org/10.1007/s10107-004-0559-y.
[36] Bürger A, Zeile C, Hahn M, Altmann-Dieses A, Sager S, Diehl M. pycombina: An open-source tool for solving combinatorial approximation problems arising in mixed-integer optimal control. IFAC-PapersOnLine 2020;53(2):6502–8, 21st IFAC World Congress.
[37] Bonami P, Biegler LT, Conn AR, Cornuéjols G, Grossmann IE, Laird CD, Lee J, Lodi A, Margot F, Sawaya N, Wächter A. An algorithmic framework for convex mixed integer nonlinear programs. Discrete Optim 2008;5(2):186–204. http://dx.doi.org/10.1016/j.disopt.2006.10.011, In Memory of George B. Dantzig.
[38] Bürger A, Zeile C, Altmann-Dieses A, Sager S, Diehl M. A Gauss–Newton-based decomposition algorithm for Nonlinear Mixed-Integer Optimal Control Problems. Automatica 2023;152:110967. http://dx.doi.org/10.1016/j.automatica.2023.110967.